Imaging ellipsometry biosensor: Basic theory, principles of operation, and applications

Haoyu Liu, Jia Shen, Wei Liu, Yu Niu, and Gang Jin

Citation: Journal of Vacuum Science & Technology B **38**, 024002 (2020); doi: 10.1116/1.5129596
View online: https://doi.org/10.1116/1.5129596
View Table of Contents: https://avs.scitation.org/toc/jvb/38/2
Published by the American Vacuum Society

JVST B
Journal of Vacuum Science & Technology B

ARTICLE

avs.scitation.org/journal/jvb

Imaging ellipsometry biosensor: Basic theory, principles of operation, and applications

Cite as: J. Vac. Sci. Technol. B 38, 024002 (2020); doi: 10.1116/1.5129596
Submitted: 30 September 2019 · Accepted: 7 January 2020 ·
Published Online: 27 January 2020

Haoyu Liu,[1,2,a)] Jia Shen,[1,2,a)] Wei Liu,[1,a)] Yu Niu,[1,b)] and Gang Jin[1,2]

AFFILIATIONS

[1]NML, Beijing Key Laboratory of Engineered Construction and Mechanobiology, Institute of Mechanics, Chinese Academy of Sciences, 15 Bei-si-huan West, Beijing 100190, China
[2]School of Engineering Science, University of Chinese Academy of Science, 19 Yu-quan Road, Beijing 100049, China

Note: This paper is part of the Conference Collection: 8th International Conference on Spectroscopic Ellipsometry 2019, ICSE.
[a)]**Contributions:** H. Liu, J. Shen, and W. Liu contributed equally to this work.
[b)]**Electronic mail:** niuyu@imech.ac.cn

ABSTRACT

The imaging ellipsometry biosensor (IEB), first proposed in 1995, has advanced from a simple concept to a powerful biosensor with high throughput, high sensitivity, high specificity, and low sample consumption. By combining the technique with surface plasmon resonance, IEBs operating under total internal reflection conditions can perform real-time multisample detection of biomolecule interactions. In this paper, the authors discuss the basic theory, principles of operation, design requirements, sensing chip modifications, methodologies and performance, and applications of IEBs.

I. INTRODUCTION

Interactions between biomolecules are essential for life. Characterization of these interactions is not only the first step toward uncovering the basis of life but also is of great medical and clinical significance.[1] As a basic characterization tool, biosensors are essential for studying key interactions, such as protein–protein, DNA–protein, and ligand–receptor interactions, that play important roles in physiological processes.[2] A typical biosensor combines a biological substrate with a physicochemical detector. Interactions between biomolecules are sensed by the biological component, and the physiochemical detector transforms the sensed interactions to detectable physical signals, such as optical, electrical, or thermal signals.[3] Among the designs of biosensors, optical biosensors are the most common in academia and industry owing to their high sensitivity and the capability for minimal disturbance and disruption to the sensed biomolecule.[4]

In general, optical biosensors may be categorized into two groups: labeled biosensors and label-free biosensors. Labeled biosensors tend to possess impressive sensitivity because the label compounds can amplify the optical signal through the use of fluorescence,[5] enzymes,[6] radioactivity,[7] nanoparticles,[8] and quantum dots.[9] For example, by introducing a fluorescent label, a labeled biosensor has the ability to perform single molecule detection.[10] Despite their huge success in the past two decades, labeled biosensors have several problems. First, the introduction of labels is time-consuming.[11] Second, the label may affect the bioactivity of the target biomolecule. Third, it is difficult to perform quantitative detection because the label will introduce a degree of inhomogeneity for the target biomolecule. Last, but not the least, not all biomolecules can accept the same label, especially in the case of small biomolecules.

To overcome these limitations, label-free biosensors have been proposed. Of these label-free biosensors, the most successful one is the biosensor based on the surface plasmon resonance (SPR) phenomenon. The SPR technique can characterize biomolecular interactions in real-time with high sensitivity and accuracy.[12] To further improve the throughput for multisample detection, SPR imaging (SPRi) has been developed by replacing the photonic detector with a charge coupled device (CCD) camera. However, the sensitivity of the biosensor based on SPR or SPRi is inferior to that of the labeled biosensor.[13]

As a phase sensitive optical technique, traditionally, ellipsometry has been used to measure the thickness and the refractive index of thin films.[14] Besides its success in the semiconductor industry,

ellipsometry was employed at an early stage to study biomolecule interactions. In 1945, Rothen, who invented the word "ellipsometry," used the technique to study the attractive forces between an antibody and an antigen.[15] In 1965, Vroman and Lukosevicius employed the technique to observe the surface activation of blood clotting in real time.[16]

To measure the lateral distribution of a complex formation over a large sample area, the imaging ellipsometer (IE) was conceived.[17] The IE technique combines optical imaging with traditional ellipsometry. The technique has been used to visualize the changes of optical properties and microstructures, such as thin films and bulk samples, and to monitor dynamic surface processes.

The concept of the imaging ellipsometry biosensor (IEB) was proposed in 1995 (Ref. 18), and after development for two decades, the IEB has advanced from a simple concept to a powerful biosensor with high throughput, sensitivity, and specificity and low sample consumption. The technique has been used to image and quantify various analytes, such as antibodies, pathogenic viruses, disease biomarkers, bacteria, and so on.[19] Furthermore, combined with SPR, a real-time IEB technique, termed total internal reflection imaging ellipsometry biosensor (TIRIEB), has been developed to study the dynamic interaction processes of antigen/antibody systems[20] and redox processes at sensing surfaces.[21]

In this paper, we review the basic theory, principles of operation, design features, methodologies, sensing chip modifications, and applications of IEBs.

II. PRINCIPLES OF THE IMAGING ELLIPSOMETRY BIOSENSOR

A. Relationship between the ellipsometry signal and the biological signal

The fundamental principle of the IEB is the same as reflection ellipsometry, namely, reflection of polarized light by a stratified planar structure as described in standard textbooks.[22] In this section, a focus is given on how to interpret the parameters of the ellipsometry signal in terms of the biological signal.

The IEB is used to image the surface mass density distribution of the protein layers absorbed at a patterned solid substrate in the grayscale, as shown in Fig. 1. When the analyte in solution interacts with a corresponding ligand, the molecules assemble into biocomplexes because of the affinity interactions. The surface mass density of the protein layer increases along with the ligand–analyte interactions, and the increase of surface mass density can be obtained through the imaging characterization process of the IE, thereby verifying quantitatively the analyte concentration in the solution.

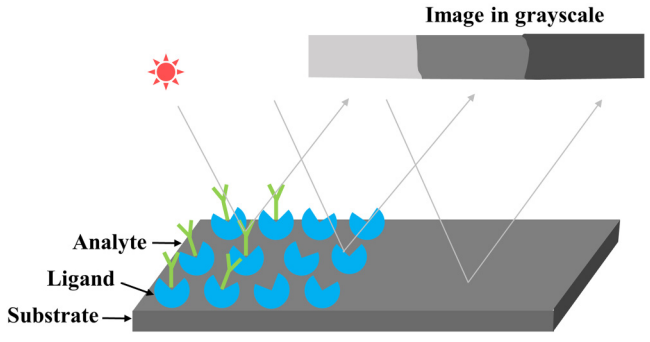

FIG. 1. Principle of IEB for detection of biomolecule interactions.

The basic measurement parameters in ellipsometry are the amplitude ψ and phase Δ of the complex reflectance ratio ρ,

$$\rho = \tan\psi e^{i\Delta} = \rho(N_0, N_1, d, N_2, \phi_0, \lambda), \tag{1}$$

where N_0, N_1, and N_2 are the refractive indices of the ambient environment, the layer, and the substrate, respectively, d is the layer thickness, ϕ_0 is the angle of incidence, and λ is the wavelength.

For biomolecule interactions, the biomolecule layer thickness is usually between 1 and 10 nm, a thickness which is below the detection capability for IEB. Thus, in the case of a fixed angle of incidence, we have

$$\delta\psi \propto \delta d, \tag{2a}$$

$$\delta\Delta \propto \delta d. \tag{2b}$$

Given that the increase of the film thickness of the protein layer δd is proportional to the surface mass density variation $\delta\Gamma$,[23] the ellipsometry parameters change with the variation in the surface mass density of the protein layer on a proportional basis,

$$\delta\psi \propto \delta\Gamma, \tag{3a}$$

$$\delta\Delta \propto \delta\Gamma. \tag{3b}$$

As IEB uses a conventional polarizer-compensator-sample-analyzer (PCSA) configuration, the signal δI may be expressed as

$$\delta I = I_0\left(\frac{\delta R_s}{R_s} + \alpha_1\delta\psi + \alpha_2\delta\Delta\right), \tag{4}$$

where I_0 is the detected light intensity for the bare substrate and R_s is the reflectance for s-polarized light. $\psi\delta$ and $\delta\Delta$ are the ellipsometric parameter variations, while α_1 and α_2 are the coefficients for $\psi\delta$ and $\delta\Delta$, respectively. The explicit expression for α_1 and α_2 is reported elsewhere.[22] For IEB, silicon (Si) or gold (Au) may serve as the substrate. Thus, R_s is insensitive to the change of film thickness on the surface, which implies $\delta R_s \approx 0$. It can be deduced that

$$\delta I \propto \delta\Gamma = \delta\gamma \cdot M, \tag{5}$$

where $\delta\gamma$ and M represent the amount of surface density of the protein layer and the protein molecular weight, respectively.

Equation (5) suggests that for a given analyte, the signal variation for IEB is proportional to the amount of surface density of the biomolecule layer; therefore, IEB may be used for monitoring biomolecules. Typical applications are outlined in Sec. V.

B. The dynamic process observed by TIRIEB

The IEB operating in the external reflection mode is concerned mainly with the equilibrium of the ligand–analyte interaction. Real-time detection provides an opportunity to sense the dynamic interaction process, which is crucial for weak affinity detection and multianalyte recognition.[24] The first design configuration to demonstrate real-time measurement was based on an external reflection IEB using an open glass cell. The sample consumption for this design was around 5 ml.[14] To reduce the amount of biological sample and avoid poor imaging quality caused by solution disturbance, the TIRIEB technique was proposed, the TIRIEB method being based on establishing the internal reflection condition and combining the SPR phenomenon with the IE technique. A detailed discussion on this topic is available elsewhere.[25] Here, we briefly review the fundamentals of the SPR phenomenon and the relationship between the TIRIEB signal and the SPR signal. Then, we will discuss the dynamic processes that may be observed by TIRIEB.

Consider the internal reflection for a glass/solution system. When the incident angle is larger than the critical angle, total internal reflection occurs. An evanescent wave emerges along the interface, and this wave decays exponentially in solution (the medium with low refractive index). The penetration distance of the evanescent wave is about 100 nm, and the distance is sensitive to a variation in the optical thickness at the interface.[26] Thus, a variation in optical thickness can be utilized to monitor the physical and chemical disturbances at the sensing surface. When an Au film of thickness about 50 nm is introduced at the interface, the intensity of the evanescent wave from the p-polarized light will be enhanced by SPR. The reflectance of the p-polarized light decreases and reaches a minimum at a specific angle, which is called the SPR angle. At the same time, the phase of the p-polarized reflection changes abruptly around the SPR angle. Working under this condition, solution disturbance will be reduced significantly. Moreover, the consumption of the biological sample can be reduced dramatically by using a microfluidic system.

The fractional change of the p-polarized reflectance and the s-polarized reflectance can be interrelated by

$$\frac{\delta R_p}{R_p} = \frac{\delta R_s}{R_s} + \frac{4\delta\psi}{\sin 2\psi}. \tag{6}$$

Therefore, according to Eq. (4), we have

$$\frac{\delta I}{I_0} = \frac{\delta R_p}{R_p} + \left(\alpha_1 - \frac{4\delta\psi}{\sin 2\psi}\right)\delta\psi + \alpha_2\delta\Delta. \tag{7}$$

Equation (7) implies that the optical signal for the TIRIEB can be categorized in two parts: the response due to SPR and the response due to the ellipsometry variation at the sample surface. By having a configuration that ensures proper alignment of the polarized light, the ellipsometry response will be such that the TIRIE signal response is at least 10 times more sensitive than that of SPR.[27,28]

Typically, there are two types of dynamic processes observed by TIRIEB: (1) the formation of ligand–analyte complexes at the sensing surface and (2) the diffusion of molecules in the neighborhood of the interface.

1. Formation of ligand–analyte complexes at the sensing surface

The recognition process involving the ligand and analyte[21] may be represented as

$$\text{ligand} + \text{analyte} \underset{k_d}{\overset{k_a}{\rightleftharpoons}} \text{ligand} \cdot \text{analyte}, \tag{8}$$

where k_a and k_d are the association rate constant and the dissociation rate constant, respectively. Thus, the equilibrium constant for the dissociation is defined as $\mathbf{K}_\mathrm{D} = k_d/k_a$. Assuming a pseudo-first order interaction, the rate equation for the formation of the ligand–analyte complex is given by

$$dc_{ligand-analyte}/dt = k_a c_{ligand} c_{analyte} - k_d c_{ligand-analyte}, \tag{9}$$

where $c_{analyte}$, c_{ligand}, and $c_{ligand-analyte}$ are the concentrations of the analyte and the ligand in solution, and the ligand–analyte complex on the sensing surface, respectively. The solution for Eq. (9) can be given by

$$c_{ligand-analyte} = \frac{c_{analyte}(\gamma_{ligand})_0 \cdot (1 - e^{-(k_a \cdot c_{analyte} + k_d)\cdot t})}{K_D + c_{analyte}}, \tag{10}$$

where $(\gamma_{ligand})_0$ is the initial amount of the ligand before the analyte solution is delivered to the substrate.

Given that $\delta\Gamma \propto c_{ligand-analyte}$, we have

$$\delta I \propto \frac{c_{analyte}(\gamma_{ligand})_0 \cdot (1 - e^{-(k_a \cdot c_{analyte} + k_d)\cdot t})}{K_D + c_{analyte}}. \tag{11}$$

Equation (11) implies that the dynamic process of the ligand–analyte complex is governed not only by the analyte concentration but also by the rates of association/dissociation. Thus, by observing the dynamic process of the variation in signal response, biomolecular interaction analysis can be performed using TIRIEB. A typical example is given in Sec. V.

2. Diffusion of molecules near the interface

The diffusion of molecules near the sensing surface will be influenced by the local refractive index. The change in refractive index[23] is given by

$$\delta N_2 \approx \sum \theta \delta C(z, t)|_{z=0}, \tag{12}$$

where $\delta C(z, t)|_{z=0}$ is the molecule concentration near the electrode and θ is the local refractive index change for the complex per unit concentration for each molecule. Furthermore, we have

$$\delta\psi \propto \delta N_2, \tag{13a}$$

$$\delta\Delta \propto \delta N_2. \tag{13b}$$

According to Eqs. (4), (12), (13a), and (13b), the optical signal

originating from molecule diffusion at the interface is given by

$$\delta I \propto \sum \theta \delta C(z, t)|_{z=0}. \quad (14)$$

Equation (14) suggests that the optical response from molecular diffusion is governed by the local concentration of the molecules. Normally, the determination of the local molecular concentration is difficult. However, under certain circumstances, the concentration may be described by Fick's second law[29] as follows:

$$\frac{\partial C}{\partial t} = D\frac{\partial^2 C}{\partial z^2}, \quad (15)$$

where C and D are the concentration and the diffusion coefficients, respectively. Using the initial boundary conditions and the given boundary conditions will provide a specific solution, which has been shown to be in agreement with the experimental results.[27]

III. SYSTEM DESIGN AND PROCEDURES

A. System design

As typical ellipsometry techniques, IEB and TIRIEB are based on a PCSA configuration as shown in Fig. 2. The light beam from a Xe lamp is extended and collimated to the polarizer. Beyond the polarizer, the linearly polarized light beam passes through a compensator (quarter wave plate) and impinges on the sample. After reflection, the light beam passes through a second polarizer, which is termed the analyzer, and strikes the detector, a CCD camera. The IEB operating in the external reflection mode is illustrated in Fig. 2(a), and the TIRIEB is depicted in Fig. 2(b).

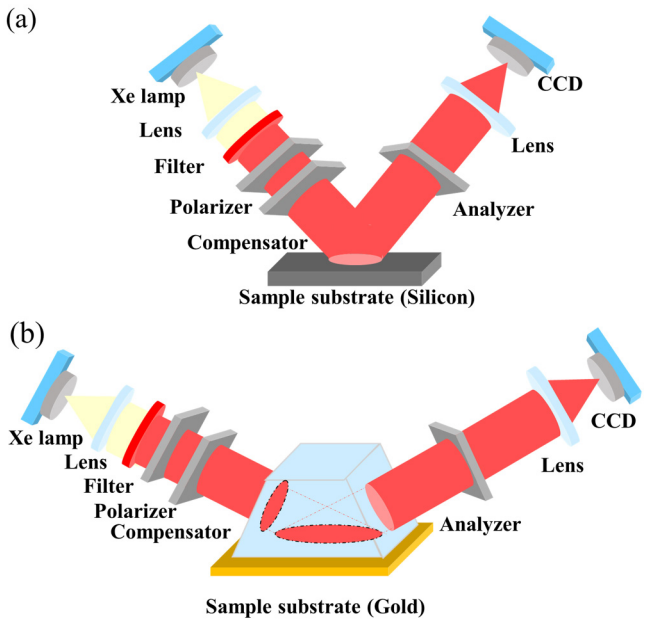

FIG. 2. Schematic illustration of (a) IEB in the external reflection condition and (b) TIRIEB. A trapezoidal prism is used to couple the detection beam to the sensing surface. The polarized collimated beam is propagated perpendicularly to the prism and onto the sensing surface.

B. Microfluidic reactor

In a traditional ellipsometry sensor, the biomolecules are spotted or printed onto the substrate surface. However, it is difficult to produce perfect spots and the procedure of spotting is time-consuming, hence the need for a fabrication technique with easier operation and low sample consumption. Microfluidic devices require much smaller reagent volumes, offer short reaction times, and give the possibility for parallel operation. The devices also hold the promise for integrating an entire measurement system onto a single chip. Therefore, a microfluidic reactor is employed in IEB.

As shown in Fig. 3, a typical reactor may have 24 independent interaction cells. Each cell (~100 nl) is attached to microtubes via an inlet and an outlet port. The inlet ports are connected by transfer tubing to sample solutions, and the outlet ports are connected to a peristaltic pump.

C. Procedures

The analytical procedures for implementing IEB consist of four steps. First, the substrate is modified by the delivery of the chemical reagents, in a process called surface modification. Then, the modified substrate is placed on the microfluidic reactor. The ligand and the target are then pumped successively onto the surface of the substrate. Finally, the ligand is combined with the target to form a biological complex for biological interaction. The whole procedure is recorded by the CCD, as illustrated in Fig. 4.

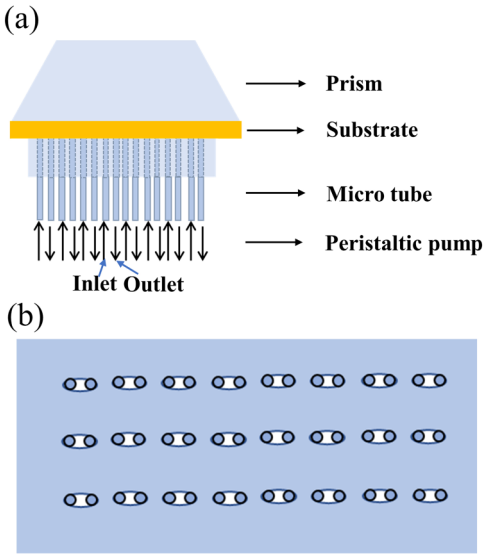

FIG. 3. Schematic of (a) microfluidic reactor and (b) microarray with 24 cells.

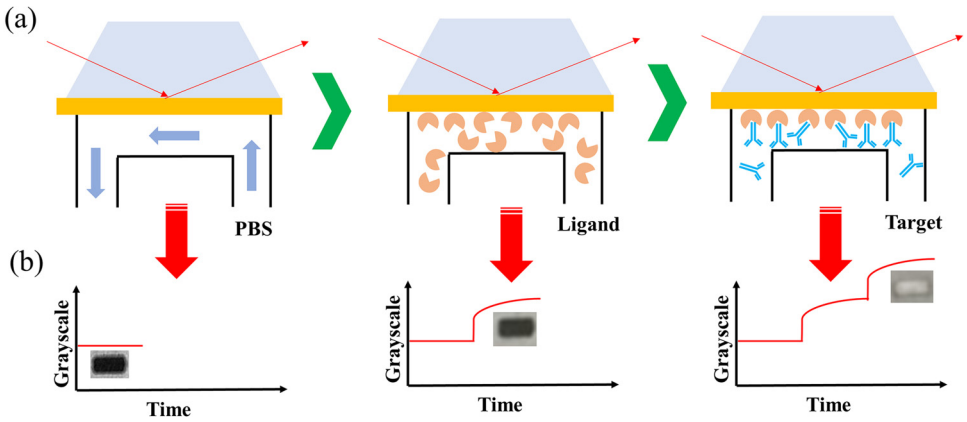

FIG. 4. Schematic of (a) phosphate buffer saline (PBS) buffer at baseline, ligand immobilization, and target detection by TIRIEB, and (b) the corresponding real-time detection signals.

IV. SENSING CHIP MODIFICATIONS

For practical applications, modifications of the sensing chip play a key role in biosensing in terms of facilitating the recognition of the target analyte and preventing nonspecific adsorption. In this section, we will summarize chip modification procedures for IEB.

A. Physical adsorption

To immobilize the ligand on the biosensor surface and prevent unspecific binding, physical adsorption was first used for the immobilization step. Silicon wafers previously etched by a piranha solution were incubated in a dichlorodimethylsilane solution to form a highly hydrophobic surface.[18,30] Through hydrophobic interactions, protein ligands were immobilized such that the sensing surface was formed. However, the immobilized proteins were prone to partial denaturation, tended to wash off the surface, and replaced with more active proteins by competitive adsorption.[31–33]

B. Covalent immobilization

To overcome the aforementioned problems, covalent immobilization was introduced whereby the proteins were immobilized via strong and stable covalent bonds. Wang and Jin modified an Si surface with 3-aminopropyltriethoxysilane (APTES), which was then activated with glutaraldehyde (GLU) to immobilize the protein covalently for IEB.[34] Later, this method was used successfully for immunoassay techniques.[35–38] Some procedures for surface modification and ligand immobilization are outlined below.

1. Silicon surface modification

There are two common methods for surface modification of an Si substrate. The first one is that the Si substrate is modified with APTES and GLU successively to fabricate a $—(CH_2)_3N═CH(CH_2)_3—CHO$ moiety for capturing amino groups of protein ligands. The other method is that the Si substrate is modified with APTES and succinic anhydride successively, and then the modified surface is activated with *N*-hydroxysuccinimide (NHS) and 1-ethyl-3-[3-dimethylaminopropyl]-carbodiimide hydrochloride (EDC) to bind the amino group of proteins.

The ligand surface concentration influences directly the amount of analyte that is captured; this aspect is important to ensure satisfactory IEB performance. To further optimize the ligand surface concentration and minimize nonspecific adsorption, methyltriethoxysilane (MTES) is mixed with APTES under various experimental conditions to modify the Si surface. The results suggest that the immobilized IgG provides better bioactivity on the APTES/MTES-GLU modified surface than the IgG on the surface without APTES/MTES-GLU.[39]

2. Au surface modification

There are two main methods for surface modification of Au. One is to prepare alkanethiol-based self-assembled monolayers (SAMs),[39–44] which can easily form a highly organized and extremely stable organic thin film at the nanometer scale with good reproducibility.[44] After an activation process with NHS or EDC, the SAMs with exposure to the carboxyl groups can be used to bind covalently with amine groups of the target proteins. To simplify the procedure, another modification is introduced, which is to immerse the Au substrate in a solution containing carbon disulfide (CS_2) and the binding protein. The CS_2 can spontaneously react with amine groups to form dithiocarbamates, which can immobilize some compounds with primary or secondary amine groups.

3. Oriented immobilization

To ensure the ligands present with an enhanced bioactivity, especially in the case of antibody ligands, oriented immobilization has been employed. Protein A can bind selectively the Fc domain of antibody molecules[45] and expose the outer Fab portion where specific recognition occurs. This feature is applied when there is a need to design a method for the oriented immobilization of antibody ligands. A hydrophobic surface may first be incubated in a solution of protein A and blocked with bovine serum albumin, and then incubated in an IgG solution to form the antibody sensing surface. Finally, anti-IgG solution is delivered to the IgG sensing surface. The amount of anti-IgG bound with IgG immobilized by protein A on the Si surface is much more than that achieved with IgG physically adsorbed on a surface, thus confirming that protein A can be used to immobilize antibody molecules in a highly

oriented manner and maintain the antibody molecular functional configuration on the Si surface with excellent reproducibility.

V. APPLICATIONS

After a period of sustained development, IEB has been applied to diverse applications, including early tumor diagnosis,[20] clinical therapy marker detection,[46] interaction affinity analysis,[34] and environmental pollution monitoring.[21]

A. Detection of disease biomarkers

Alpha-fetoprotein (AFP), alpha-L-fructosidase (AFU), and ferritin are important liver tumor biomarkers. Jin *et al.* have designed a liver tumor biomarker joint detection system for AFP, AFU, and ferritin as indicated in Fig. 5.[20,47] First, protein A is assembled on a carboxyl modified Si surface. Then, the antibodies for AFP, AFU, and ferritin are immobilized on the modified Si surface. In addition, standard samples of AFP, AFU, and ferritin covering several concentrations are used to prepare a calibration curve for IEB. The detection ranges for AFP, AFU, and ferritin are from 1 to 64 ng/ml and 5 to 160 ng/ml. The ROC (receiver operating characteristic) curve analysis suggests that simultaneous measurement of AFP and AFU is a more reliable measure for liver biomarker status than measurement of the individual biomarkers.

For clinical analysis of low molecular weight proteins in serum, a sandwich strategy has been introduced. One such example is the determination of procalcitonin (PCT), a 13 kDa protein which is a blood infection biomarker used for guiding antibiotic therapy;[48] the method in question is approved by the Food and Drug Administration (FDA, USA). Li *et al.* have designed an analytical strategy based on a sandwich structure, employing a capture antibody (cAb)–analyte–detection antibody (dAb).[46] The cAb is first immobilized on the substrate to capture the analyte and then the dAb is introduced. Instead of employing direct analyte detection, the analytical strategy relies on the analyte concentration being sensed as a result of the signal variation occurring in the dAb layer. Not only is the detection signal of the IEB amplified but also the nonspecific adsorption due to the serum is avoided. The analytical procedure is outlined in Fig. 6(a). The limit of detection (LOD), deduced from the calibration data, is 0.081 ng/ml [see Fig. 6(b)], confirming that IEB can perform serological analysis for PCT with good analytical performance.

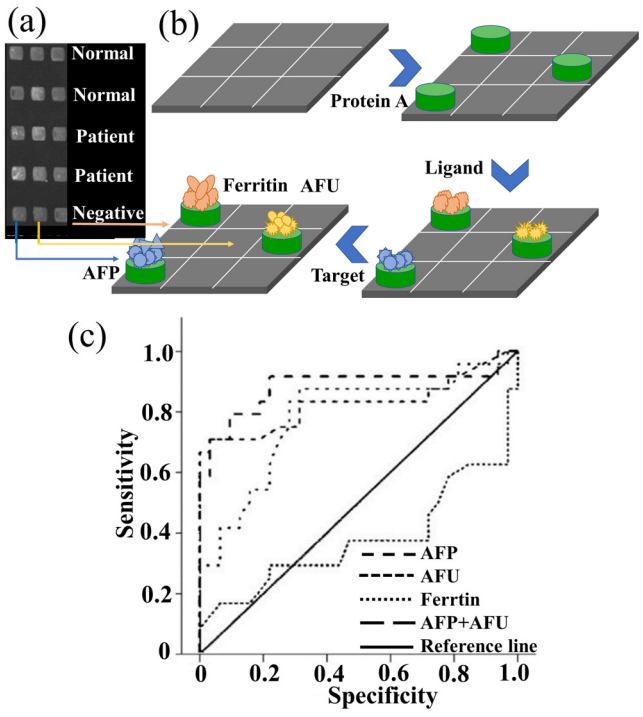

FIG. 5. (a) Example of joint detection image of AFP, AFU, and ferritin. Two normal sera, two patient sera, and one negative control are detected simultaneously. (b) Schematic for design of the surface process. (c) The ROC curve analysis for AFP, AFU, ferritin, and AFP and AFU. The areas under the curve (AUCs) are 0.827, 0.782, and 0.380 for AFP, AFU, and ferritin, respectively, while the AUC for joint detection of AFP and AFU is 0.884. Reprinted with permission from Jin *et al.*, Thin Solid Films **519**, 2750 (2011). Copyright 2011, Elsevier.

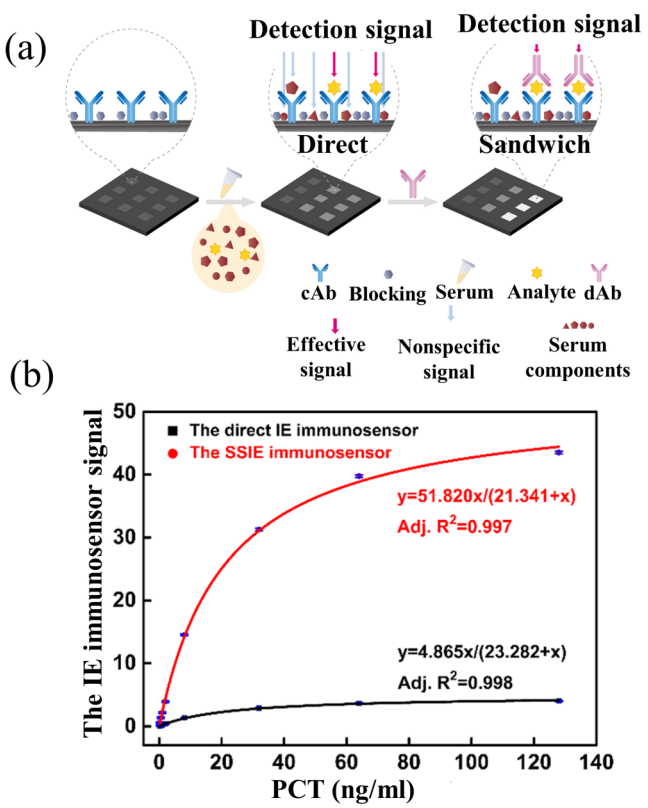

FIG. 6. (a) Schematic of the design process for surface detection of procalcitonin in serum by IEB. (b) The calibration curve for measuring PCT by IEB. Reprinted with permission from Li *et al.*, Anal. Chem. **90**, 8002 (2018). Copyright 2018, American Chemical Society.

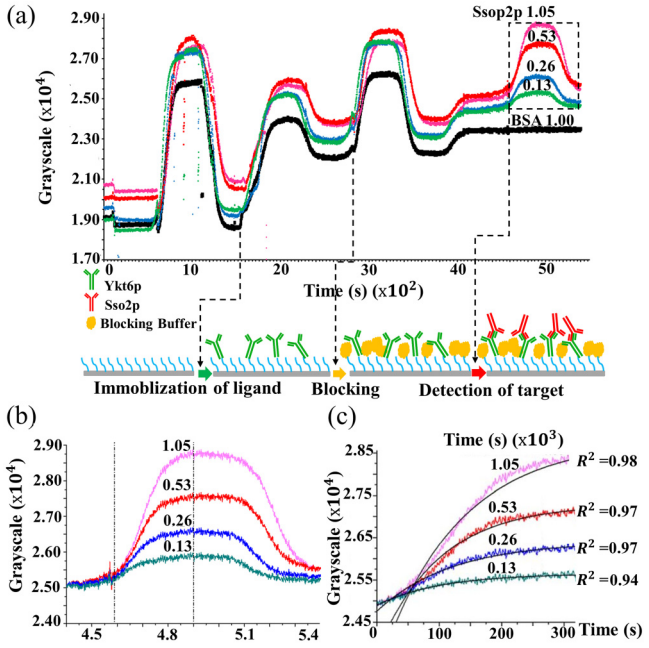

FIG. 7. (a) Real-time curves for various concentrations of Sso2p interacting with Ykt6p as measured by TIRIEB and a schematic of the design process for surface detection of Sso2p. (b) The amplified real-time binding curves of SNARE interactions measured by TIRIEB. (c) Best fits for the association phase of the real-time binding curves for calculating the kinetic constants. Reprinted with permission from Qi *et al.*, Sci. Rep. **4,** 5341 (2014). Copyright 2014, Springer Nature.

B. Biomolecule interaction analysis

Biomolecule interactions control all types of biological phenomena, such as neural signal transduction,[49] immunological reactions,[50] attachment of enzymes to substrates,[51] and so on. Kinetic analysis of biomolecule interactions, especially the weak affinity interactions that usually reflect transient processes, assists in obtaining kinetic parameters and revealing the laws governing life processes.[52]

The soluble *N*-ethylmaleimide–sensitive factor attachment receptor (SNARE) proteins (Sec22p, Ykt6p, and Sso2p) are a family of proteins that mediate membrane fusion during cell fusion or cellular trafficking.[53] The qualitative and quantitative identifications of SNARE interactions are the key to understanding the mechanisms of fusion events. In 2014, as depicted in Fig. 7, Qi *et al.* used an IEB to identify the weak interactions between SNARE proteins and provide kinetic constants for the binding and dissociation.[54] The kinetic constants are listed in Table I.

C. Environmental pollution monitoring

IEB is applicable not only to clinical analysis but also to environmental measurement. Dissolved oxygen (DO) is an important parameter for assessing water quality because of its influence on organisms in natural waters.[55] Without sufficient DO, fish and aquatic animals cannot survive. Traditionally, an electrochemical sensor, the Clark electrode, has been used to monitor the redox status of DO. However, the consumption of the electrode material causes signal drift. To overcome this problem, TIRIEB has been developed to monitor DO reduction in waters[21,56] as illustrated in Fig. 8; the detection limit is 2–8 mg/l as shown in Fig. 9.[56] By introducing an amplification medium, such as a surface tethered weak polyelectrolyte, i.e., polyaniline with iron-porphyrin, the LOD for DO was improved tenfold relative to that for the unmodified surface without the amplification medium.

TABLE I. Kinetic analysis and constants for Ykt6p, Sec22p, and Sso2p by TIRIEB. The constants for the interactions include the association rate constant (k_a), the dissociation rate constant (k_d), the association constant (K_A) ($K_A = k_a/k_d$), and the dissociation constant (K_D) ($K_D = k_d/k_a$). Reprinted with permission from Qi *et al.*, Sci. Rep. **4,** 5341 (2014). Copyright 2014, Springer Nature.

Ligand/target	k_a ($M^{-1}S^{-1}$)	k_d (S^{-1})	K_A ($10^4\,M^{-1}$)	K_D (10^{-5} M)
Sso2p/Ykt6p	336.5 ± 62.6	0.0051 ± 0.001 3	6.7 ± 1.3	1.5 ± 0.54
Sso2p/Sec22p	351.0 ± 50.2	0.006 ± 0.002	6.3 ± 1.6	01.7 ± 0.4
Ykt6p/Sso2p	285.5 ± 13.6	0.0053 ± 0.000 57	5.4 ± 1.3	1.9 ± 0.21
Sec22p/Sso2p	572.0 ± 13.4	0.0075 ± 0.000 44	7.7 ± 1.9	1.4 ± 0.4

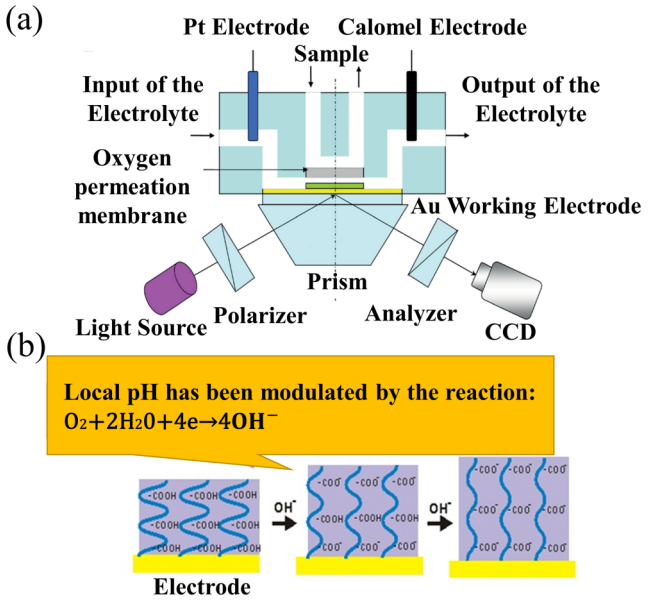

FIG. 8. (a) Schematic of the TIRIEB used for total internal reflection imaging ellipsometry and electrochemistry measurement. Polyaniline (the rectangle on the Au Working Electrode) modified Au layer (30 nm) was deposited on the base of an SF10 glass slide as the working electrode for simultaneous electrochemical and optical measurements. Reprinted with permission from Li *et al.*, Electroanalysis **26**, 374 (2014). Copyright 2014, John Wiley and Sons. (b) Local *p*H modulation by the dissolved oxygen reduction would elongate the carboxylated poly(OEGMA-r-HEMA) moiety. Reprinted with permission from Liu *et al.*, J. Electrochem. Soc. **163**, H286 (2016). Copyright 2016, IOP Publishing.

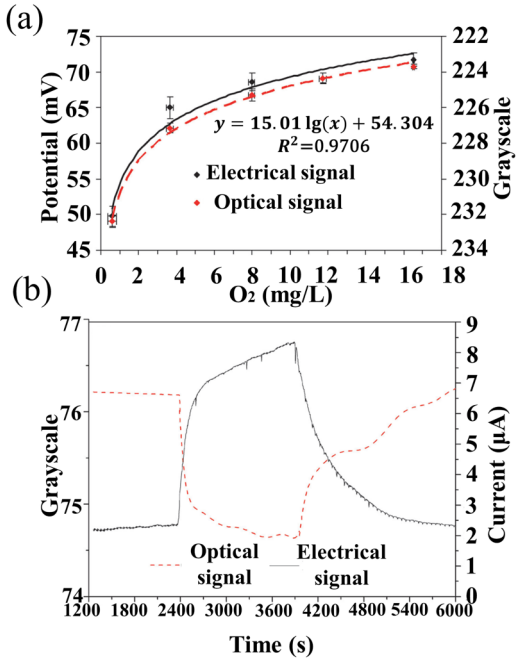

FIG. 9. (a) Open circuit potential (the solid line) and gray scale (the dashed line) responses for the EC-TIRIE sensor with a polyaniline modified Au surface for various oxygen concentrations. (b) Saturated DO reduction at the Au covered sensing surface (the solid line is the electrical signal, while the dashed line is the optical signal). Reprinted with permission from Li *et al.*, Electroanalysis **26**, 374 (2014). Copyright 2014, John Wiley and Sons.

VI. CONCLUSION AND PERSPECTIVE

Since its inception in 1995, IEB has advanced from a simple concept to a powerful biosensor detection platform for many target analytes. Phase sensitive imaging ellipsometry provides high sensitivity, high throughput, and multisample detection. The microfluidic system reduces sample consumption from the milliliter to the microliter level. Modification of the sensing chip can increase the specificity and avoid nonspecific adsorption effects. Furthermore, combined with the SPR phenomenon, TIRIEB may be used to study in real time the dynamic interactions of ligand–analyte complexes and molecule diffusion at the sensing surface. However, for trace analysis of small molecules, the sensitivity for IEB remains an issue. To improve measurement sensitivity, three strategies can be adopted: (1) introduction of comparative adsorption, (2) introduction of nanoparticles to amplify the optical signal,[57] and (3) noise suppression of the system. Furthermore, for online testing, the size of IEB should be reduced and a compact IEB should be brought to market.

ACKNOWLEDGMENTS

The authors acknowledge the financial support from the Youth Innovation Promotion Association of the Chinese Academy of Sciences (No. 2017026), the National Natural Science Foundation of China (NNSFC) (No. 81872584), the National Basic Research Program of China (No. 2015CB352100), and the International Science & Technology Cooperation Program of China (No. 2015DFG32390).

REFERENCES

[1]A. A. Kornyshev and S. Leikin, J. Chem. Phys. **108**, 7035 (1998).
[2]D. D. Dudgeon, S. N. Shinde, T. Y. Shun, J. S. Lazo, C. J. Strock, K. A. Giuliano, D. L. Taylor, P. A. Johnston, and P. A. Johnston, Assay Drug Dev. Technol. **8**, 437 (2010).
[3]F. S. Ligler and J. J. Gooding, Anal. Chem. **91**, 8732 (2019).
[4]P. Gruber, M. P. C. Marques, N. Szita, and T. Mayr, Lab Chip **17**, 2693 (2017).
[5]P. Anand, A. Fu, S. H. Teoh, and K. Q. Luo, Biotechnol. Bioeng. **112**, 1673 (2015).
[6]T. Fodey, G. Murilla, A. Cannavan, and C. Elliott, Anal. Chim. Acta **592**, 51 (2007).
[7]G. J. Gao, L. Fan, H. M. Lu, and Y. J. Hua, Chin. Sci. Bull. **53**, 1675 (2008).
[8]C. Y. Lee, L. P. Wu, T. T. Chou, and Y. Z. Hsieh, Sens. Actuators B Chem. **257**, 672 (2018).
[9]R. Wilson, D. G. Spiller, A. Beckett, I. A. Prior, and V. See, Chem. Mater. **22**, 6361 (2010).
[10]Q. T. Easter and S. A. Blum, Acc. Chem. Res. **52**, 2244 (2019).
[11]Y. Liu, H. B. Zhou, Z. W. Hu, G. X. Yu, D. T. Yang, and J. S. Zhao, Biosens. Bioelectron. **94**, 131 (2017).
[12]J. Homola, Anal. Bioanal. Chem. **377**, 528 (2003).
[13]I. Mannelli, V. Courtois, P. Lecaruyer, G. Roger, M. C. Millot, M. Goossens, and M. Canva, Sens. Actuators B Chem. **119**, 583 (2006).
[14]H. Arwin, Thin Solid Films **313**, 764 (1998).
[15]A. Rothen, Rev. Sci. Instrum. **16**, 26 (1945).
[16]L. Vroman and A. Lukosevicius, Nature **204**, 701 (1964).
[17]A. H. Liu, P. C. Wayner, and J. L. Plawsky, Appl. Opt. **33**, 1223 (1994).
[18]G. Jin, P. Tengvall, I. Lundstrom, and H. Arwin, Anal. Biochem. **232**, 69 (1995).
[19]Y. Niu and G. Jin, Protein Cell **2**, 445 (2011).
[20]G. Jin, Y. H. Meng, L. Liu, Y. Niu, S. Chen, Q. Cai, and T. J. Jiang, Thin Solid Films **519**, 2750 (2011).
[21]W. Liu, M. Li, B. Lv, Y. Y. Chen, H. W. Ma, A. S. Viana, J. P. Correia, and G. Jin, J. Electrochem. Soc. **163**, H286 (2016).
[22]R. M. A. Azzam and N. M. Bashara, *Ellipsometry and Polarized Light* (Elsevier Science, New York, 1987).
[23]H. Arwin, S. Welin-Klintström, and R. Jansson, J. Colloid Interface Sci. **156**, 377 (1993).
[24]Z. H. Wang and G. Jin, Anal. Chem. **75**, 6119 (2003).
[25]Y. Y. Chen, Z. H. Wang, Y. H. Meng, and G. Jin, Int. J. Nanotechnol. **4**, 171 (2007).
[26]J. Homola, Chem. Rev. **108**, 462 (2008).
[27]L. Liu, Y. Niu, S. Chen, Y. H. Meng, H. W. Ma, and G. Jin, Sci. Chin. Phys. Mech. **53**, 1805 (2010).
[28]L. Liu and G. Jin, "Total internal reflection imaging ellipsometry (TIRIE) biosensor sensitivity improvement with low noise imaging device," Proc. SPIE **7875**, 78750U (2011).
[29]L. P. Tang and J. Gulikers, Cem. Concr. Res. **37**, 589 (2007).
[30]Z. H. Wang and G. Jin, J. Biochem. Biophys. Methods **57**, 203 (2003).
[31]S. K. Bhatia, L. C. Shriverlake, K. J. Prior, J. H. Georger, J. M. Calvert, R. Bredehorst, and F. S. Ligler, Anal. Biochem. **178**, 408 (1989).
[32]L. C. Shriver-Lake, B. Donner, R. Edelstein, K. Breslin, S. K. Bhatia, and F. S. Ligler, Biosens. Bioelectron. **12**, 1101 (1997).
[33]L. Vroman, A. L. Adams, G. C. Fischer, and P. C. Munoz, Blood **55**, 156 (1980).
[34]Z. H. Wang and G. Jin, J. Immunol. Methods **285**, 237 (2004).
[35]C. M. Halliwell and A. E. G. Cass, Anal. Chem. **73**, 2476 (2001).

[36]J. N. Lin, J. Herron, J. D. Andrade, and M. Brizgys, IEEE Trans. Biomed. Eng. **35**, 466 (1988).
[37]M. Yoshioka, Y. Mukai, T. Matsui, A. Udagawa, and H. Funakubo, J. Chromatogr. Biomed. **566**, 361 (1991).
[38]H. D. Yuan, W. M. Mullett, and J. Pawliszyn, Analyst **126**, 1456 (2001).
[39]M. Frasconi, F. Mazzei, and T. Ferri, Anal. Bioanal. Chem. **398**, 1545 (2010).
[40]W. H. Hu, Z. S. Lu, Y. S. Liu, and C. M. Li, Langmuir **26**, 8386 (2010).
[41]A. Ulman, Chem. Rev. **96**, 1533 (1996).
[42]W. Limbut, P. Kanatharana, B. Mattiasson, P. Asawatreratanakul, and P. Thavarungkul, Biosens. Bioelectron. **22**, 233 (2006).
[43]J. C. Love, L. A. Estroff, J. K. Kriebel, R. G. Nuzzo, and G. M. Whitesides, Chem. Rev. **105**, 1103 (2005).
[44]K. L. Prime and G. M. Whitesides, Science **252**, 1164 (1991).
[45]I. Bjork, B. A. Petersso, and J. Sjoquist, Eur. J. Biochem. **29**, 579 (1972).
[46]Y. K. Li, W. Liu, G. Jin, Y. Niu, Y. P. Chen, and M. X. Xie, Anal. Chem. **90**, 8002 (2018).
[47]Y. Niu, T. F. Kang, and G. Jin, Thin Solid Films **571**, 453 (2014).
[48]H. B. Reith, U. Mittelkotter, E. S. Debus, C. Kussner, and A. Thiede, Dig. Surg. **15**, 260 (1998).
[49]R. Schliebs, Int. J. Dev. Neurosci. **24**, 87 (2006).
[50]E. M. Rodilla, I. D. Gonzalez, E. L. Yges, F. J. M. Bellido, M. T. G. Bare, and F. L. Toledano, Expert Rev. Clin. Immunol. **6**, 789 (2010).
[51]M. Malmqvist, Nature **361**, 186 (1993).
[52]T. F. Kang, Y. Niu, and G. Jin, Thin Solid Films **571**, 463 (2014).
[53]A. Joshi, H. Garg, S. D. Ablan, and E. O. Freed, J. Biol. Chem. **286**, 29861 (2011).
[54]C. Qi, H. Zhang, L. Liu, R. K. Yang, T. F. Kang, W. X. Hao, G. Jin, and T. J. Jiang, Sci. Rep. **4**, 5341 (2014).
[55]D. H. Zhao, S. Palanisamy, and S. M. Chen, Int. J. Electrochem. Sci. **10**, 10038 (2015).
[56]M. Li, W. Liu, J. P. Correia, A. C. Mourato, A. S. Viana, and G. Jin, Electroanalysis **26**, 374 (2014).
[57]Z. Wang *et al.*, Anal. Chem. **91**, 6769 (2019).